

Picosecond Mid-IR Laser Induced Surface Damage on Gallium Phosphate (GaP) and Calcium Fluoride(CaF₂)

Ho Lee*

School of Mechanical Engineering, KyungPook National University, 1370 Sankyuckdong Bukgu, Daegu 702-701, Korea

(Manuscript Received June 16, 2006; Revised February 1, 2007; Accepted April 19, 2007)

Abstract

Picosecond mid-IR USPL induced surface damage on a Gallium Phosphate (GaP) and Calcium Fluoride (CaF₂) is reported. A semiconductor GaP and a dielectric material CaF₂, that are transparent over 3~10 μ m, were exposed to one picosecond mid-IR light (4.7 μ m) to investigate laser-induced surface morphological changes on the target. The initiation of damage along the polishing scratch line of GaP and the random location of damage digs on the CaF₂ suggests that the mid-IR picosecond laser-induced damage on targets started from intrinsic surface defects. Multiple pulse irradiations produced periodic corrugated surface structures (ripples) perpendicular to the polarization of light on both GaP and CaF₂. In terms of the orientation and the spacing between ripples, observed ripples have common features with previously reported ripples.

Keywords: Ultra short pulse laser; Laser machining; Incubation effect; Laser-induced ripple

1. Introduction

An ultrashort pulse laser (USPL) emits pulses with duration less than the time required for an energy exchange between electrons and material lattices (Kittel, 1996). Typical heat diffusion time from absorbing electrons/lattices to the neighboring lattices in metal is a few picoseconds and that in semiconductors and dielectrics is in the range of tens or hundreds of picoseconds. Due to its short pulse duration, the interaction between USPL and material can be highly localized, allowing us to (1) achieve more precise ablation, (2) minimize thermal and mechanical damage to the surrounding region, and (3) avoid interaction between the laser pulse and the ablated plume (Chichkov, 1996; Neev, 1996; Oraevsky, 1996; Stoian, 2000). These advantages over longer pulsed lasers have generated significant interest

for potential application of USPL in many fields, including pulsed laser deposition of thin films (Vasquez, 1999), machining (Chang, 2004), and biomedical applications. It has been reported that ablation using near IR (wavelength up to 1064nm) USPL is initiated by multiphoton ionization, followed by electron avalanche. As a consequence, ablation threshold and ablation rate are less sensitive to the linear absorption of the material, and may be governed by a nonlinear interaction between the laser pulse and material. Most previous studies involving the USPL focused on the near IR USPL ablation.

The interaction between the mid-IR laser with matter has been an interesting topic, since the development of the Free Electron Laser (wavelength: 3 μ m~30 μ m, the macropulse width ~3 μ sec). That is because most polymers and the biological tissues have linear absorption peaks in the mid-IR regime. The interaction between the matter and mid-IR USPL has not been studied due to the lack of a laser source. A separate paper had reported on the mechanism of

*Corresponding author. Tel.: +82 53 950 5572
E-mail address: holee@knu.ac.kr

the mid-IR USPL induced breakdown (Simanovskii, 2003). In this paper, picosecond mid-IR USPL induced surface damage on a Gallium Phosphate (GaP) and Calcium Fluoride (CaF_2) is reported. A semiconductor GaP and a dielectric material CaF_2 were exposed to the one picosecond mid-IR light ($4.7\mu\text{m}$) to investigate laser-induced surface morphological changes on the target. The initiation of surface damage and the periodic surface structure on both materials are reported.

2. Methodology

An amplified optical parametric amplifier (OPA) was employed as the laser source for ablating targets. This laser can generate a picosecond pulse with energy of $60\mu\text{J}$ over the mid-infrared spectrum ($4\text{--}8\mu\text{m}$) with a repetition rate of 10 Hz and pulse duration of 1 ps . One of the drawbacks of the employed OPA system is that the output power can dramatically decrease due to the absorption of water vapor in the ambient air. A wavelength of $4.7\mu\text{m}$ was chosen for the experiment, because the absorption of water vapor at $4.7\mu\text{m}$ is lower than other wavelengths.

A semiconductor GaP and a dielectric material CaF_2 , were selected as targets. Both of them are typically used as the optical windows for mid-IR and transparent for $4.7\mu\text{m}$. The surface quality of GaP and CaF_2 is specified as 60/40 (scratches/digs) and 40/20, respectively. Mid-IR transparent materials were selected to eliminate the effect of linear absorption during the laser-target interaction.

A linearly polarized laser beam was focused on the material surface using a concave and a convex mirror (Fig. 1). Beam diameters were measured by a knife-edge method at the focal spot. Measured beam diameters were $12\mu\text{m}$. The pulse energy was monitored with an energy probe and a joule meter that received a fraction of the laser pulse reflected from a beam splitter. Surface morphological changes after a single pulse and a sequence of pulses were observed by using optical and electron microscopes. The single

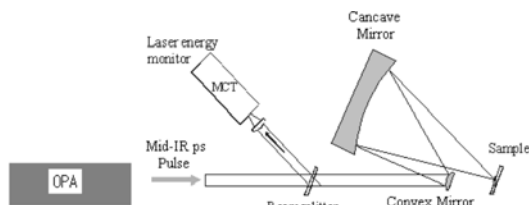


Fig. 1. A schematic diagram of the experiment.

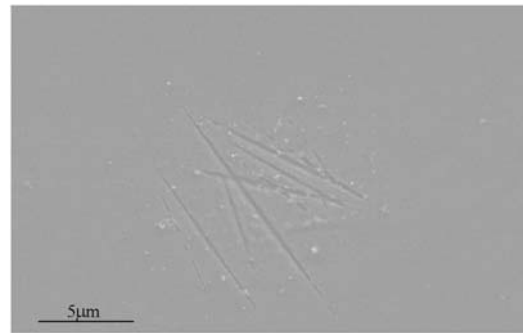
pulse-induced damage threshold was defined as any surface modification detectable under optical and electron microscopes.

3. Results

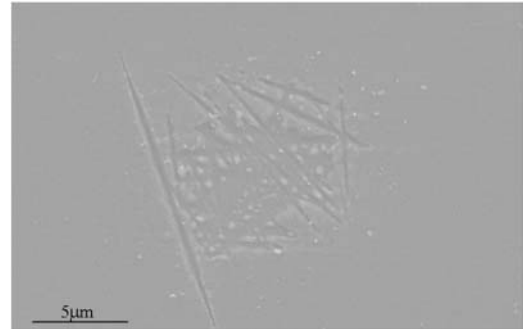
3.1 Surface damages on gallium phosphate

3.1.1 Single pulse induced damage.

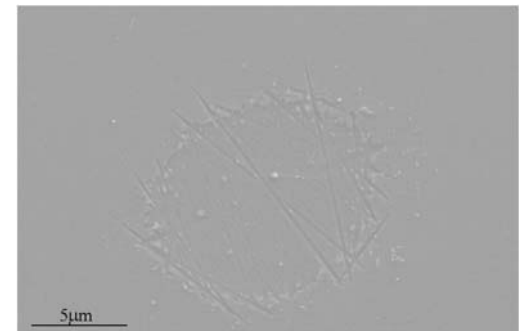
Single pulse-induced damage threshold fluences (F_{th}) for GaP measures 1.2 J/cm^2 . Typical SEM images of single pulse-induced surface damage on GaP are presented in Fig. 2. The fluences are normalized by



(a) $F/F_{\text{th}}=1.1$



(b) $F/F_{\text{th}}=2.2$



(c) $F/F_{\text{th}}=4.0$

Fig. 2. Single pulse induced surface damage on GaP. F/F_{th} is the fluence normalized by the damage threshold fluence.

the damage threshold fluence (F/F_{th}). Near the damage threshold fluence, a single pulse created randomly oriented trenches that are believed to be along previously non-visible polishing scratches [Fig. 2 (a)]. As fluence increases, the damage expands from the initial trench to the neighboring region [Fig. 2 (b)]. With the highest fluence tested, laser-induced damage develops over the whole laser spot, causing it to look as if a thin layer in the middle is ablated, which visualizes the edge of the spot [Fig. 2 (c)].

3.1.2 Multiple pulse-induced damage

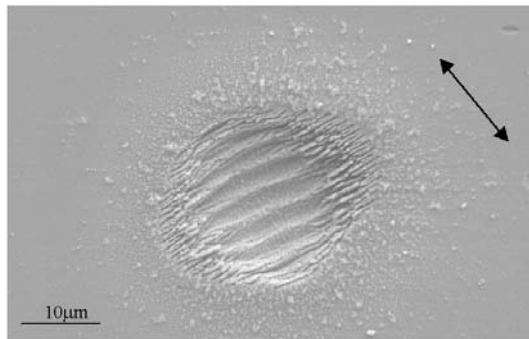
With normalized fluence (F/F_{th}) of 2.0~4.0, multiple pulse (typically 50~100 pulses) irradiations on GaP produced periodic corrugated surface structures (ripples) perpendicular to the polarization of light. Figure 3 provides typical examples of these ripples. Arrows indicate the polarization of the incident laser. The periodicities (the spacing between ripples) of

ripples are approximately $3.5 \mu\text{m}$.

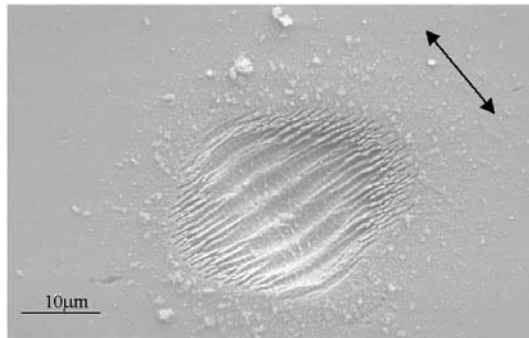
3.2 Surface damage on calcium fluoride

3.2.1 Single pulse induced damage

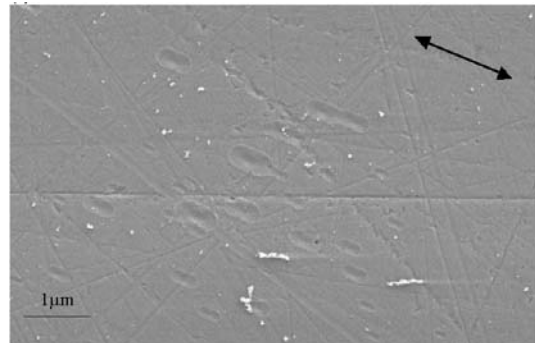
Single pulse-induced damage threshold fluences (F_{th}) for GaP measures 6.5 J/cm^2 . Typical SEM images of single pulse-induced surface damage on CaF_2 are presented in Fig. 4. The fluences are normalized by the damage threshold fluence (F/F_{th}). Near the damage threshold fluence, a single pulse made small digs that were randomly distributed over the whole laser spot [Fig. 4(a)]. As fluence increased, the number of digs increased [Fig. 4(b)]. It should be emphasized that these digs were elongated along the polarization of the beam. They measure approximately $1 \mu\text{m}$ and accompany the re-deposition of melt material. Polishing scratches on CaF_2 should be distinguished from those on GaP, since scratches on CaF_2 were visible prior to the laser irradiation.



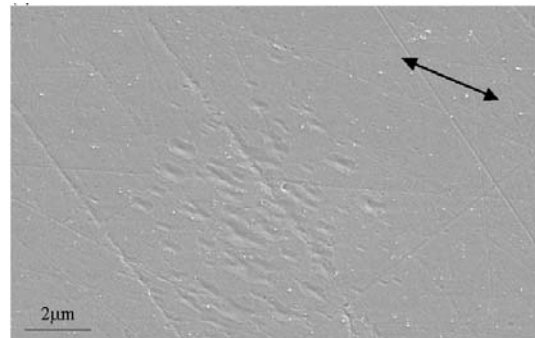
(a) $F/F_{th}=2.2$, Number of pulses: 100 pulses



(b) $F/F_{th}=4$, Number of pulses: 50 pulses



(a) $F/F_{th}=1.1$



(b) $F/F_{th}=1.3$

Fig. 3. Multiple pulse induced periodic surface structure on GaP. F/F_{th} is the fluence normalized by the damage threshold fluence. The arrow indicates the polarization of the incident light.

Fig. 4. Single pulse induced surface damage on CaF_2 . F/F_{th} is the fluence normalized by the damage threshold fluence. The arrow indicates the polarization of the incident light.

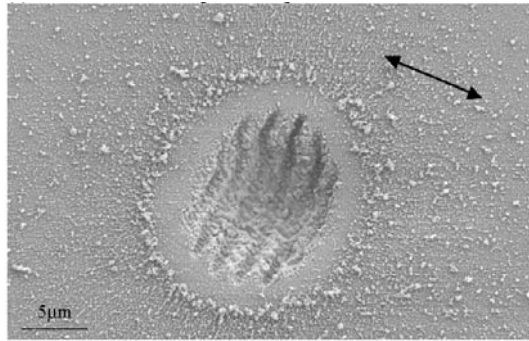
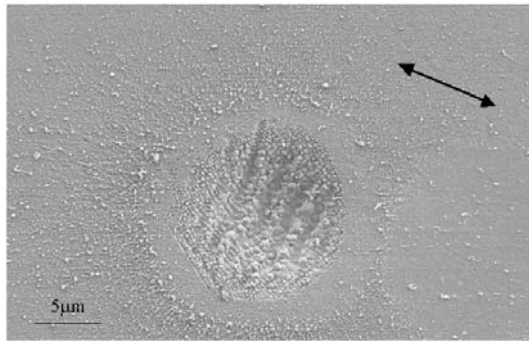
(a) $F/F_{th}=1.3$, Number of pulses: 50 pulses(b) $F/F_{th}=2.0$, Number of pulses: 20 pulses

Fig. 5. Multiple pulse induced periodic surface structure on CaF_2 . F/F_{th} is the fluence normalized by the damage threshold fluence. The arrow indicates the polarization of the incident light.

3.2.2 Multiple pulse-induced damage

With normalized fluence (F/F_{th}) of 1.3~2.0, multiple pulse (typically 50~100pulses) irradiations on CaF_2 produced ripples perpendicular to the polarization of light. Typical examples of these ripples are shown in Fig. 5. Arrows indicate the polarization of the incident laser. The periodicities (the spacing between ripples) are about $2.5 \mu\text{m}$.

In case of irradiation of more than 300 pulses, the laser produced bulk material removal (Fig. 6), and the bulk material removal occasionally accompanied chippings at the rim of the crater.

4. Discussion

Figures 2 and 5 suggest that the mid-IR picosecond laser-induced damage on GaP and CaF_2 started from the intrinsic surface defects. Intrinsic surface defects, such as digs and scratches, on the surface dramatically reduce the damage threshold energy, since they enhance the absorption efficiency by introducing

additional energy states between conduction and covalence bands. This phenomenon is called *incubation effect* and the surface defects are referred to as *incubation centers* (Baurele, 2000a; Koehner, 2000; Ashkenasi, 1997; Stoian, 2000). Upon the irradiation of the laser pulse, the electric field is enhanced around the incubation center. This results in the onset of laser-induced surface damage. Once the laser-induced damage starts around the incubation center, the damage expands around it.

A single pulse irradiation produced randomly oriented lines on GaP Fig. 2(a). These lines are considered to be the damage along the polishing scratches that were not observable prior to the laser pulse. The laser-induced damage made the polishing lines visible as if it engraved scratches on the surface. The damage digs on CaF_2 (Fig. 4) also suggest the incubation effect. The damage spot consists of a large number of small digs elongated in the direction of the laser electrical field vector (polarization). Randomly located digs, associated with “weak” points on the surface served as incubation centers.

Particularly interesting is the elongated shape of these digs. The elongation of the digs has been explained in a separate paper based on the breakdown mechanism and can be summarized as follows (Simanovskii, 2003). It is generally accepted that the USPL-induced breakdown in the solid is initiated by the generation of seed electrons by either multiphoton ionization (MPI) or tunneling ionization (TI). Once seed electrons are generated, they collide with nearby unexcited electrons. Through this collision process, the number of free electrons is multiplied (avalanche ionization), eventually forming dense plasma. The relative role of these ionization processes depends on the material properties and on the pulse duration and wavelength.

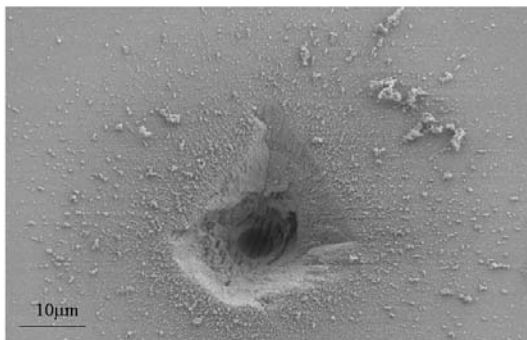
Upon the irradiation of mid-IR USPL, the tunnelling ionization alone leads to the dense plasma formation on the semiconductors. On the other hand, the plasma on the dielectric materials is initiated by a combination of the tunneling ionization and the avalanche ionization. The drifting of electrons associated with the avalanche ionization on the CaF_2 is considered as the cause of the elongation. As the free electrons travel within the electric circuit, the laser-induced free electrons can be drifting within an electric field of the laser. The observed elongation is attributed to the drifting along the electric field (the polarization) of the laser. The drift distance estimated

for the applied electric field (laser fluence) is a fraction of $1 \mu\text{m}$, which corresponds quite well to the length of elongated digs.

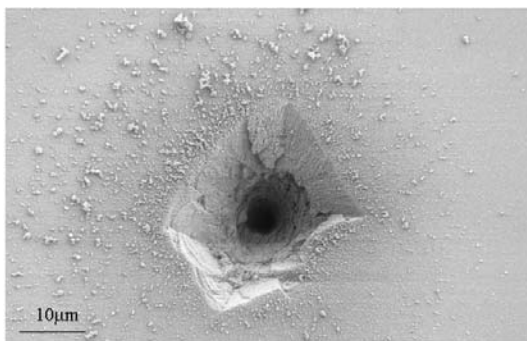
Once the damage initiated around the intrinsic defects, the laser produced bulk material removal with additional pulses. The bulk material removal occasionally accompanied chippings at the rim of the crater (Fig. 6). The chippings around the craters indicate that laser-induced photomechanical effects are strong enough to produce fractures around the crater. The photomechanical effect can be initiated separately by two different processes or a combination of both. First, the rapid temperature increase at the surface induces the thermoelastic expansion that results in the escalation of the shear stress (Oraevsky, 1997). Initiation of fracture occurs when this shear stress exceeds the local tensile strength. Secondly, the photomechanical effect can be initiated due to the laser-induced plasma. Once the plasma forms, the plasma expands through the absorption of the laser pulse. The rapid expansion of plasma induces a shock wave that causes the additional bulk

material removal (Gusev, 1993).

Laser-induced ripples, as shown in Figs. 3 and 5, have been widely observed and studied, since Birnbaum first observed them after irradiating semiconductors with a ruby laser with irradiance of $10^4\sim 10^5 \text{ W/cm}^2$ (Birnbaum, 1965). It has been postulated that these coherent structures (termed ‘laser-induced ripple’) on the surface are induced by a standing wave that is produced by the interference of incident, reflected and/or scattered light by the microscopic non-uniformity of the target surface (Baurele, 2000b; Akhmanov, 1985; Keilmann, 1982). The standing wave results in the spatially periodic laser intensity on the target surface. This non-homogenous energy deposition induces spatially periodic melting and re-solidification, leading to the corrugated structures (ripples). These ripples on various materials including metal, semiconductor and insulator are characterized by two features. (1) The spacing between ripples (periodicity) is in the order of the wavelength and increases with the wavelength. (2) The orientation of laser induced ripples is mainly perpendicular to the polarization of laser, while under certain conditions ripples are parallel to the polarization. The periodicity of observed ripples on GaP and CaF_2 is about $2\sim 3 \mu\text{m}$ which is similar to the wavelength of the incident light. The ripple orientation is perpendicular to the polarization of the incident laser. These suggest that mid IR picosecond pulse-induced ripples on GaP and CaF_2 have similar features with previously reported ripples produced with different laser parameters (wavelength and pulse duration).



(a) $F/F_{\text{th}}=1.33$, Number of pulses: 300 pulses



(b) $F/F_{\text{th}}=2.0$, Number of pulses: 300 pulses

Fig. 6. Multiple pulse induced deep crater and chips on CaF_2 . F/F_{th} is the fluence normalized by the damage threshold fluence.

5. Conclusion

We have examined mid IR picosecond laser-induced surface morphological changes on GaP and CaF_2 . The initiation of damage along the polishing scratch line of GaP and the random location of damage digs on the CaF_2 suggests that the mid-IR picosecond laser-induced damages on targets started from the intrinsic surface defects. Once the damage was initiated around the intrinsic defects, the laser produced deep craters with additional pulses. The bulk material removal occasionally accompanied chips at the rim of the crater.

Multiple pulse irradiations produced periodic corrugated surface structures (ripples) perpendicular to the polarization of light on both GaP and CaF_2 . In

terms of the orientation and the spacing between ripples, observed ripples have common features with previously reported ripples on different materials with distinct laser parameters.

Acknowledgement

This research was supported by Kyungpook National University Research Fund, 2006

References

- Akhmanov, S. A., Emel'yanov, V. I., Koroteev, N. I. and Seminogov, V. N., 1985, "Interaction of Powerful Laser Radiation with the Surfaces of Semiconductors and Metals: Nonlinear Optical Effects and Nonlinear Optical Diagnostics," *Soviet physics: Uspekhi*, Vol. 28, pp. 1084~1124.
- Ashkenasi, D., Rosenfeld, A., Varel, H., Wahmer, M. and Campbell, E. E. B., 1997, "Laser Processing of Sapphire with Picosecond and Sub-Picosecond Pulses," *Applied Surface Science*, Vol. 120, pp. 65~80.
- Baurele, D., 2000a, *Laser processing and chemistry*, Chapter 12, Berlin, Springer.
- Baurele, D., 2000b, *Laser processing and chemistry*, Chapter 21, Berlin, Springer.
- Birnbaun, M., 1965, "Semiconductor Surface Damage Produced by Ruby Lasers," *Journal of Applied Physics*, Vol. 36, pp. 3688-3689.
- Chang, W., Choi, M., Kim, J., Cho, S. and Whang, K., 2004, "Nanoscale Patterning Using Femtosecond Laser and Self-Assembled Monolayers(SAMs)," *Journal of Korean Society of Mechanical Engineering*, Vol. 28, pp. 1270~1275.
- Chichkov, B. N., Momma, C., Nolte, S., von Alvensleben, F. and Tunnermann, A., 1996, "Femtosecond, Picosecond and Nanosecond Laser Ablation of Solids," *Applied Physics A*, Vol. 63, pp. 109~115.
- Gusev, V. E. and Karabutov, A. A., 1993, *Laser Optoacoustics*, New York: AIP Press.
- Keilmann, F. and Bai, Y. H., 1982, "Periodic Surface Structures Frozen into CO₂ Laser-Melted Quartz," *Applied Physics A*, Vol. 29, pp. 9~18.
- Kittel, C., 1996, *Introduction to solid state physics*, 7th ed., Wiley, New York.
- Koechner, W., 2000, *Solid State Laser Engineering*, Chapter 11, Berlin, Springer.
- Neev, J., Da Silva, L. B., Feit, M. D., Perry, M. D., Rubenchik, A. M. and Stuart, B. C., 1996, "Ultrashort Pulse Lasers for Hard Tissue Ablation," *IEEE Journal of Selected Topics in Quantum Electronics*, Vol.2, pp. 790~800.
- Oraevsky, A. A., Da Silva, L. B., Rubenchik, A. M., Feit, M. D., Glinsky, M. E., Perry, M. D., Mammini, B. M., Small, W. IV and Stuart, B. C., 1996, "Tissues With Nanosecond-to-Femtosecond Laser Pulses: Relative Role of Linear and Nonlinear Absorption," *IEEE Journal of Selected Topics in Quantum Electronics*, Vol. 2, pp. 801~809.
- Oraevsky, A. A., Jacques, S. L. and Tittel, F. K. "Measurements of Tissue Optical Properties by Means of Time-Resolved Detection of Laser-Induced Transient Stress," *Applied Optics*, Vol. 36, pp. 402~415.
- Simanovskii, D., Schwettman, H. A., Lee, H. and Welch, A. J., 2003, "Mid-Infrared Optical Break-down in Dielectrics," *Physical Review Letters*, Vol. 91, No. 10, 107601(1-4).
- Spooner, G. J. R., Juhasz, T., Traub, I. R., Djotyan, G., Horvath, C., Sacks, Z., Marre, G., Miller, D. and Williams, A. R., 2000, "Commercial and Biomedical Applications of Ultrafast Lasers," *Proceedings of SPIE*, Vol. 3934, pp. 62~72.
- Stoian, R., Ashkenasi, D., Rosenfeld, A., Wittmann, M., Kelly, R. and Campbell, E. E. B., 2000, "The Dynamics of Ion Expulsion in Ultrashort Pulse Laser Sputtering of Al₂O₃," *Nuclear Instruments and Methods in Physics Research B*, Vol. 166~167, pp. 682~690.
- Vasquez, M. J., Halada, G. P., Clayton, C. R. and Gouma, P. I., 1999, "Fabrication of Nanostructured Al CuMg Thin Film by Femtosecond Pulsed Laser Ablation," *Thin Solid Films*, Vol. 458, pp. 37~42.